

ARMY RESEARCH LABORATORY



Investigation of Geometric Effects on the SMARTweave Signal

by Clarissa J. DuBois, William O. Ballata,
and Shawn M. Walsh

ARL-TR-1675

May 1998

19980707 119

Approved for public release; distribution is unlimited.

The findings in this report are not to be construed as an official Department of the Army position unless so designated by other authorized documents.

Citation of manufacturer's or trade names does not constitute an official endorsement or approval of the use thereof.

Destroy this report when it is no longer needed. Do not return it to the originator.

Army Research Laboratory

Aberdeen Proving Ground, Maryland 21005-5069

ARL-TR-1675**May 1998**

Investigation of Geometric Effects on the SMARTweave Signal

Clarissa J. DuBois, William O. Ballata, Shawn M. Walsh
Weapons and Materials Research Directorate, ARL

Abstract

SMARTweave or Sensors Mounted As Roving Threads is an electrical grid comprised of orthogonal noncontacting conductive filaments used primarily to monitor the resin flow in the manufacturing of liquid-molded composite materials. It works on the principles of the half Wheatstone bridge and ionic mobility. It has been successfully demonstrated as a technology, but now the challenge is to characterize the system and its behaviors. The variables addressed in this report are basically geometric in nature. The following will each be investigated: the sensor materials and their perpendicular area of conduction, the separation from one node to the next in the horizontal plane, and the separation from one lead to the next in the vertical plane. Results are presented regarding the SMARTweave sensor materials and signals. The results on horizontal spacing, the area of conduction, and vertical separation will be presented.

Table of Contents

	<u>Page</u>
List of Figures	v
List of Tables	vii
1. Introduction	1
2. SMARTweave System	1
3. SMARTweave Sensor Materials and Signals	5
4. Horizontal Separation Distance	7
4.1 Resistivity of Resin - Experimental Methods	7
4.2 Effective Area of Sensor Material - Experimental Methods	10
4.3 Results and Discussion	11
4.3.1 <i>Voltage vs. Time</i>	11
4.3.2 <i>Hole Diameter vs. Resistance</i>	12
4.3.3 <i>Effective Area Comparison</i>	14
5. Sensor Area	14
5.1 Experimental Methods	15
5.2 Results and Discussion	16
5.3 Vertical Separation Distance	16
5.3.1 <i>Experimental Methods</i>	16
5.3.2 <i>Results and Discussion</i>	17
6. Conclusions	17
7. Future Work	18
Distribution List	19
Report Documentation Page	31

INTENTIONALLY LEFT BLANK.

List of Figures

<u>Figure</u>	<u>Page</u>
1. SMARTweave Circuit Diagram	2
2. Hot Buttons Initial SMARTweave Screen	3
3. The Faces Option That Allows the User to Define the Size of the Grid and/or Multiple Faces	3
4. The Flow Screen (6 × 6 Face), Where the Data Acquisition, Recording, and Display Takes Place	4
5. The Replay Screen, Where Previously Recorded Data Can Be Replayed and Analyzed	5
6. The SMARTweave Signal Differences for Various Sensor Materials	6
7. Concentric Aluminum Cylinder Resistivity Cell (ASTM Standard D4496 [10.02]) Used to Determine Volumetric Resistivity	8
8. Double Y Plot, Showing the Relationship of Voltage and Resistance	9
9. Voltage of SMARTweave Signal for Several Different Hole Diameters	12
10. Resistance as Measured by the Cu Sensors in the Varying Hole Diameters	13
11. A Schematic of an Experiment to Determine the Effect of Differing Cross-Sectional Areas	15
12. Degradation of Signal as the Area of Conduction Is Reduced	16

INTENTIONALLY LEFT BLANK.

List of Tables

<u>Table</u>	<u>Page</u>
1. Resistivity Values of Derakane 411-C50/0.02 Weight-Percent CoNap Found Using Resistivity Cell and SMARTweave Portable System	10
2. Amount of Resin Added to Each Hole Size of Effective Area Comparison	11
3. Comparison of the SMARTweave Signal at Varying Hole Diameters for the Different Sensor Materials	13

INTENTIONALLY LEFT BLANK.

1. Introduction

SMARTweave or Sensors Mounted as Roving Threads is an electrical grid comprised of orthogonal noncontacting conductive filaments used primarily to monitor the resin flow in the manufacturing of liquid-molded composite materials. It works on the principles of the half Wheatstone bridge and ionic mobility. It has been successfully demonstrated as a technology, but now the challenge is to characterize the system and its behaviors. The variables addressed in this report are basically geometric in nature. The following will each be investigated: the sensor materials and their perpendicular area of conduction, the separation from one node to the next in the horizontal plane, and the separation from one lead to the next in the vertical plane. To begin, the SMARTweave system will be described in detail. Second, SMARTweave sensor materials and signals will be discussed. Next, the research on horizontal spacing, the area of conduction, and vertical separation will be presented. Finally, conclusions based on the results will be drawn.

2. SMARTweave System

The SMARTweave system consists of two planes of conductive threads in an orthogonal noncontacting grid. The two layers are separated by the permeable, yet insulative, plies of the fabric preform. A 12-V direct current (DC) signal is sent through one of the planes of sensors, which are called "excitation lines." The polymeric resin material, which serves as the matrix for the composite, contains ions that are free to move within the fluid. SMARTweave uses this fact; therefore, as the resin fills the preform, the two planes of sensors form a series of connected circuits through the impregnated composite. The second plane of sensors measures the voltage that can cross the gap between the two planes, called "sense lines." Figure 1 depicts the general circuit schematic for the SMARTweave system. Since a direct current is used, only the ionic mobility of the resin is being measured.

The SMARTweave system consists not only of the electrical sensing grids but also a series of hardware and software components. First, the excitation unit, which was custom-made for the U.S.

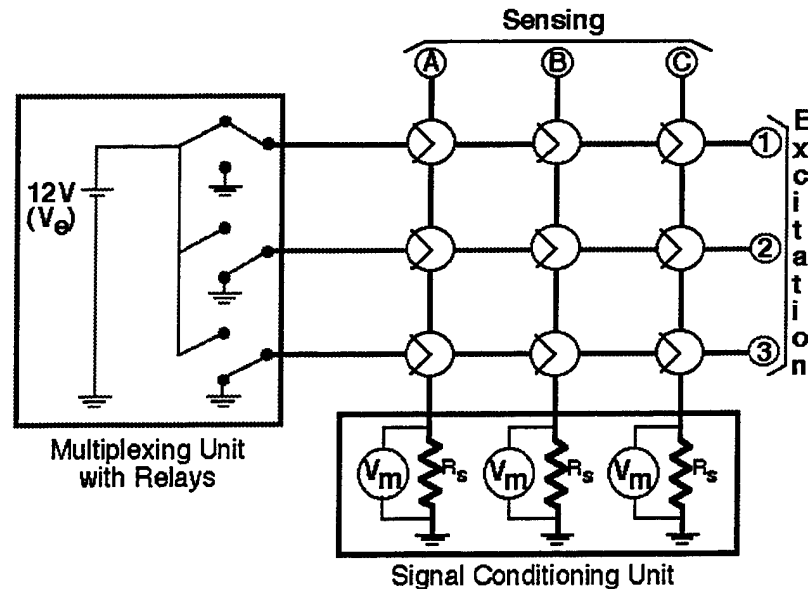


Figure 1. SMARTweave Circuit Diagram. This Is the Generalized Circuit of How the SMARTweave System Operates.

Army Research Laboratories by Waibel Technical Computing (WTC), contains the 12-V DC power supply, as well as mechanical relays used to switch from one excitation line to another. A National Instruments SCXI-1000 Chassis with a 1,300 module controls the sense lines. A Dolch L-PAC 586 portable computer is used to collect and analyze the data. Finally, the SMARTweave software program was written by WTC on National Instruments LabVIEW Version 3.0. Sixteen sense and 16 excitation lines were made of shielded cable, all of which had 1-in copper (Cu) alligator clips as connectors. Each excitation and sense line was assigned a number from 0 to 15. All intersecting lines were then labeled according to their nodal coordinates (i. e., sense no., excitation no.). All data were taken and recorded to correspond to this ranking.

The user is faced with five main options upon entering the SMARTweave software package, as depicted in Figure 2. The sampling rate may be defined in the grid or flow screen. At this point, the system has a maximum capacity of a 16-excitation by 16-sense line for a total of 256 nodal locations. However, not all sensors must be used at once. In the faces option, the user may define not only the number of sensors to be used to collect data but also the geometry of the grid orientation. Figure 3 illustrates the faces screen seen by the operator. In this case, an 8×8 grid has been chosen.

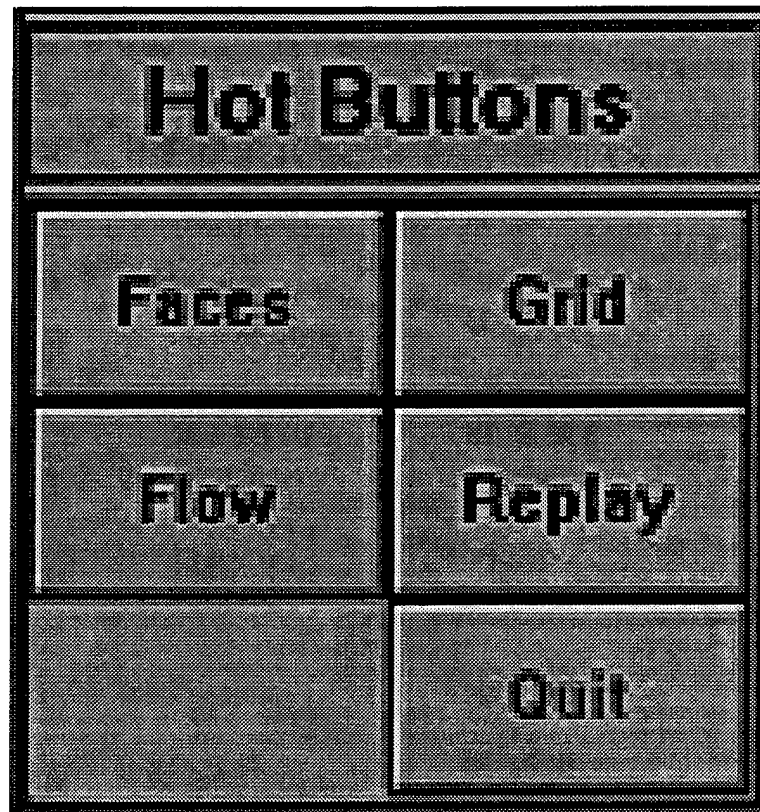


Figure 2. Hot Buttons Initial SMARTweave Screen.

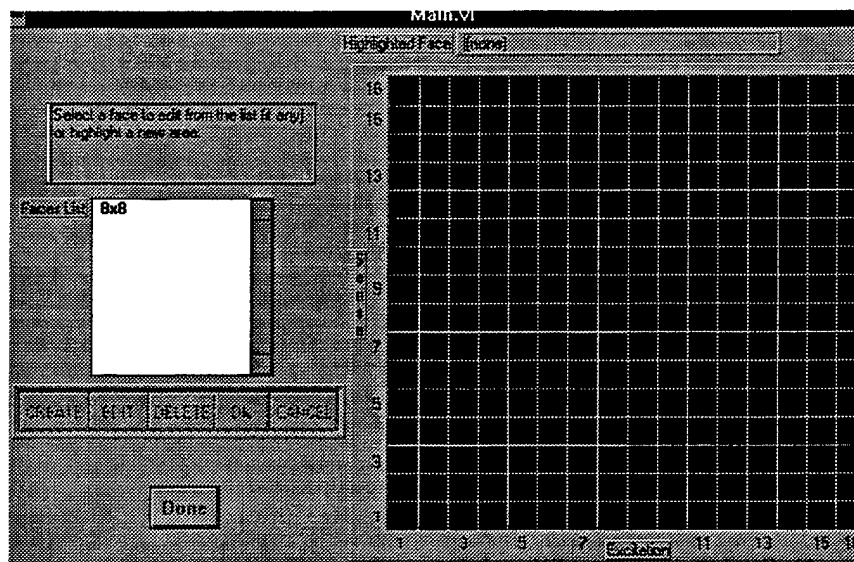


Figure 3. The Faces Option That Allows the User to Define the Size of the Grid and/or Multiple Faces.

In the flow screen depicted in Figure 4 (6×6 face), each block corresponds to a specific voltage at the respective node. The flow front of the resin may be depicted on this flow graph. Not only can one view the overall picture of the resin infusion but also one may focus upon the voltage value at individual nodes using the grid probe. The cure graph displays real-time, voltage-vs.-time data for any series of user-defined node combinations. The logging period or scan rate, file name, and elapsed time are also recorded. The elapsed time may be defined to correlate with any zero time, such as initial point of infusion or addition of the catalyst in order to judge time until gelation. Once the data have been recorded, the portable system has the option of replaying the data at any time. Figure 5 shows the replay screen, which has many of the same features as the flow screen, including overall flow, grid probe, and cure graph. In this example, a center point infusion and vacuum source, along the last excitation line, was tested. SMARTweave monitored the semicircular flow pattern induced by the experimental setup, using glass preform and a vinyl ester resin. The data may also be exported in text format with a defined amount of data points. Another feature of the replay screen is the ability to view thermal profiles recorded using a series of thermocouples, which are independent of the SMARTweave grid.

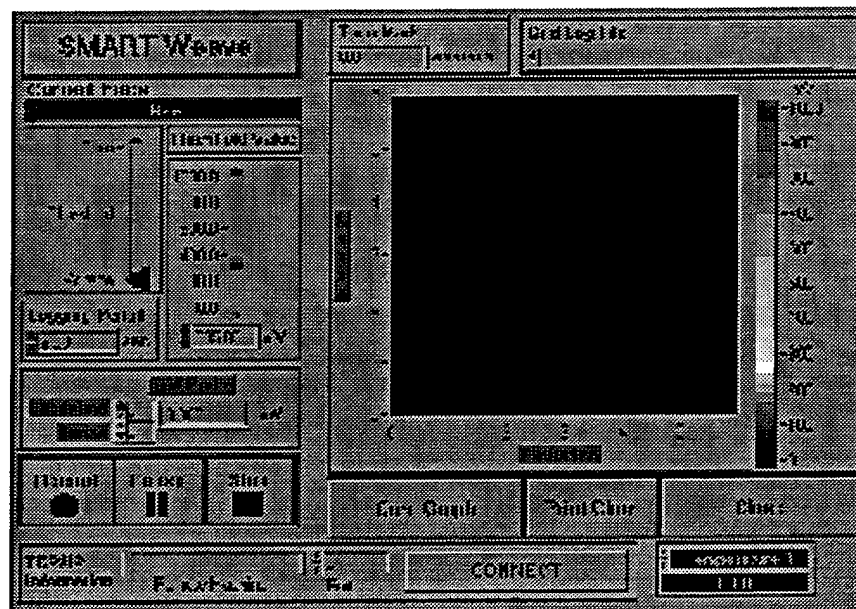


Figure 4. The Flow Screen (6×6 Face), Where the Data Acquisition, Recording, and Display Takes Place.

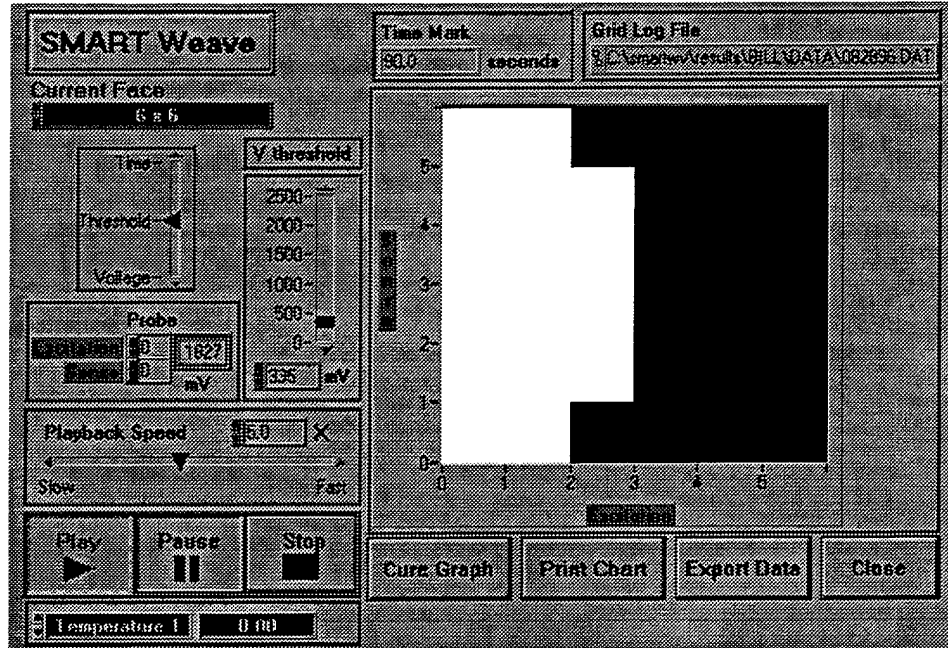


Figure 5. The Replay Screen, Where Previously Recorded Data Can Be Replayed and Analyzed.

This entire package was entitled the “portable SMARTweave system.” This was because it is completely portable and can be checked as luggage and brought to any location.

3. SMARTweave Sensor Materials and Signals

In order for SMARTweave to sense a voltage signal, the fluid between the grid must be conductive. By measuring the ionic mobility of the fluid, the relative voltage across the node junction was measured. The magnitude of the final SMARTweave signal is not only dependent upon the conductivity of the resin system but also upon the individual sensor’s material and geometry. Figure 6 depicts the SMARTweave signal of the four different sensor types tested: a 0.25-in-wide stainless steel mesh, a 4k carbon tow, 28-gauge bare Cu wire, and 0.020-in bare stainless steel wire. All trials were conducted in the same 0.75-in hole with 5 ml of Derakane 411-C50/0.02 weight-percent CoNAP, a cobalt naphthlate salt solution, and a constant separation distance of 0.105 in. As shown above, the voltage appears to be a function of the type of material and area of

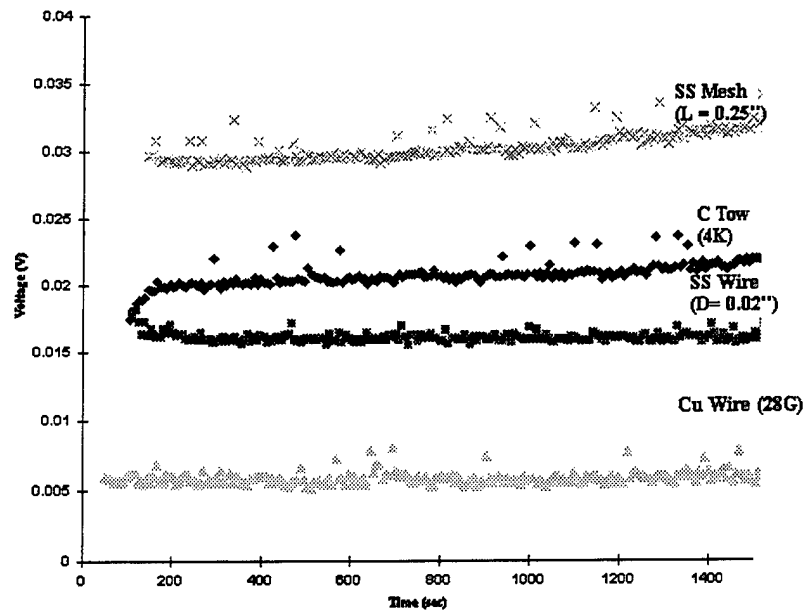


Figure 6. The SMARTweave Signal Differences for Various Sensor Materials.

the sensor. It has also been shown that both horizontal and vertical sensor separation influence the voltage signal. By isolating each of these variables, their individual effect on the magnitude of the SMARTweave signal was determined.

Numerous sensor types have been tested for use in the SMARTweave grid. These include 28-gauge bare Cu wire; 28-gauge bare Cu wire wrapped in finely braided E-glass; E-glass wrapped with a thread of Cu wire; 0.02-in stainless steel wire; 4, 8, 12, 16, and 20k unsized and sized carbon tows; 0.125-, 0.25-, and 0.50-in stainless steel mesh; and a 0.06-in graphite line. The sensors for this study were chosen based upon the following criteria in order of importance: (1) strength of SMARTweave signal, (2) economical considerations: cost/length and cost of lay-up labor, (3) reactivity in resin system, (4) change of conductivity per length before and after fluid infiltration, (5) change of material properties with sensor in place, (6) damage detection opportunities, and finally, (7) grid spacing flexibility.

4. Horizontal Separation Distance

The horizontal interactions of four sensor materials were tested: 0.25-in-wide stainless steel mesh, a 4k carbon tow, 28-gauge bare Cu wire, and 0.020-in stainless steel wire. In order to isolate each sensor's effective area

$$R/(r_v l) = A_{\text{eff}}, \quad (1)$$

the resistivity, r_v , of the noncuring (Dow's Derakane 411-C50/0.2 weight-percent Mahogany's CoNAP) and curing resin (Dow's Derakane 411-C50/2.0 weight-percent Akzo's Trigonox 239A/0.2 weight-percent Mahogany's CoNap) systems was determined.

4.1 Resistivity of Resin - Experimental Methods. First, an aluminum resistivity cell was machined according to ASTM Standard D4496 (10.02), as shown in Figure 7. Tacky tape was wrapped around a Teflon washer in order to seal the bottom of the resistivity cell. A 500-ml master batch of the uncatalyzed resin was used to do the experiment; it consisted of Dow's Derakane 411-C50, and 0.2 weight-percent CoNap was prepared (520.0-g vinyl ester, 1.06-g CoNap [a Metler 240 balance was used to mass samples]) and stored under dark conditions at room temperature. The resin was inserted into the test cell in a circular pattern using a 10-cm³ syringe with a 20-gauge syringe tip to prevent air from being trapped between the walls of the cell. Node (0,0) of the SMARTweave system was attached to the screws in the resistivity cell with Cu alligator clips to measure the voltage drop across the cell for all trials. An 8-s time interval between voltage readouts was selected. The recorded voltage data are an average over the elapsed time. A Keithley 617 electrometer was used to verify the voltage readings from the portable SMARTweave system. At this point, the nomenclature used is defined as:

A_{eff} = Effective nodal area [=] m².

D = Diameter of stainless steel wire [=] in.

D_1 = Diameter of inside cylinder of resistivity cell [=] in.

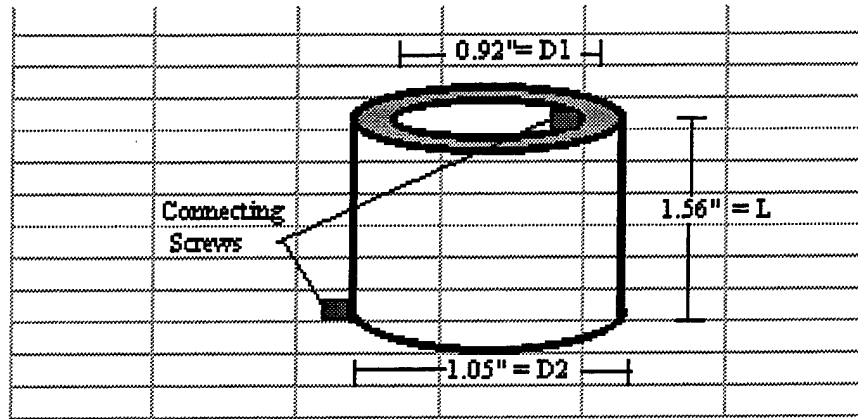


Figure 7. Concentric Aluminum Cylinder Resistivity Cell (ASTM Standard D4496 [10.02]) Used to Determine Volumetric Resistivity.

D_2 = Diameter of outside cylinder of resistivity cell [=] in.

l = Vertical separation distance [=] in.

L = Height of resistivity cell [=] in.

R = Resistance [=] Ωm .

R_j = Junction resistance [=] Ωm .

R_v = Volumetric resistance between cylinders of resistivity cell [=] Ωm .

V_D = Drop voltage [=] V.

V_e = Excitation voltage [=] V.

r_v = Volumetric resistivity [=] Ωm .

With the voltage data and dimensions of the cell, the volumetric resistivity was calculated.

$$r_v = [2pLR_v]/[\ln (D_1/D_2)] , \quad (2)$$

where D_1 = the diameter in inches of the inside cylinder, D_2 = the diameter of the outer cylinder in inches, and L = the height of the resistivity cell, also in inches. The drop voltage or V_D was then converted into a resistance through:

$$R_j = [(V_e R_D)/V_D] - R_D. \quad (3)$$

The excitation voltage or V_e remained constant at 12 V. A 10-MW drop resistor R_D was used. For the resistivity cell, the volumetric resistance, R_v , was assumed to equal the junction resistance, R_j .

$$R_v = R_j \quad (4)$$

Characteristic measured voltages and calculated junction resistances can be found in Figure 8. Both values depict a sharp change initially. Before the voltage is excited through the cell, the ions in the resin are in an equilibrium state. However, after the resin has been excited, the ions, primarily the cobalt free radical, migrate toward the negatively charged wall of the cell. The cobalt ion's migration cause the sharp increase in voltage and decrease in resistance. The leveling of the curve occurred as the ions reached a new equilibrium state. An average of the junction resistances was taken as the slope of V_D vs. time (~ 0 mV/s) until the end of the trial. The final averaged volumetric resistivity equaled $7.00 \times 10^6 \Omega\text{m}$ as calculated in Table 1.

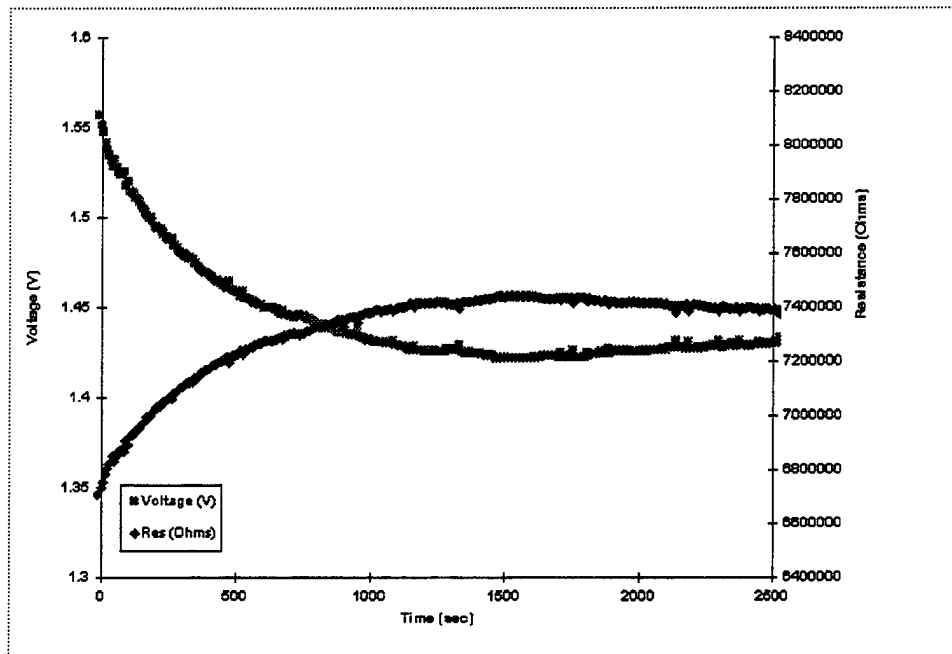


Figure 8. Double Y Plot, Showing the Relationship of Voltage and Resistance.

Table 1. Resistivity Values of Derakane 411-C50/0.02 Weight-Percent CoNap Found Using Resistivity Cell and SMARTweave Portable System

Trial	Resistivity (Ωm)	Standard Deviation (Ωm)
1	7.42E + 06	1.40E + 04
2	6.55E + 06	9.00E + 03
3	7.03E + 06	9.50E + 03
Average	7.00E + 06	1.08E + 04

4.2 Effective Area of Sensor Material - Experimental Methods. With the calculated volumetric resistivity, the junction resistance was related to the actual vertical separation distance, l , of the SMARTweave grid and the effective area, A_{eff} , of each node.

$$R = r_v (l / A_{\text{eff}}) \quad (5)$$

The area in this case is not necessarily the actual nodal area, but rather extends larger than the node. The charge did not necessarily travel in a straight path perpendicularly from the excitation line to the sense line. Therefore, the area determined is better defined as an effective area, covering a wider portion of the actual sensor. Holes ranging from 0.25 to 3.0 in at 0.25-in increments were drilled in uniformly thick composite plates. The composite plates were rinsed before and after each trial with acetone to remove any residue. The noncuring master batched resin from the resistivity trials was used for all tests. The excitation leads were attached flush to the top of the plate. A wall of tacky tape was used to surround the hole and prevent any resin leakages. The sense leads were adhered to the bottom of the plate with tacky tape, and the entire plate was sealed with a layer of vacuum bagging. The diameter of the layer of tacky tape on the top was determined so that there would be an equal amount of resin above and below each of the sensor leads. After baseline was established on the voltage-vs.-time graph of the SMARTweave system, the master batched resin was inserted. Table 2 lists the hole diameters with their respective volume of uncured resin.

Table 2. Amount of Resin Added to Each Hole Size of Effective Area Comparison

Hole Diameter (in)	Resin Volume (ml)
0.25	5
0.50	5
0.75	5
1.00	5
1.25	5
1.50	8
1.75	15
2.00	18
2.75	20
3.00	20

4.3 Results and Discussion.

4.3.1 Voltage vs. Time. As the hole diameter increased, the total sensor surface area exposed to the resin also increased. Since the magnitude of the signal is related to the mobility of the ions in the resin system, in this case the Cobalt ions, a greater surface area drawing the ions toward or pushing them away would cause an increased probability for the ions to move across from the excitation line to the sense line. Therefore, as the hole diameter increases, the SMARTweave signal increases, as shown in Figure 9. The voltage was constant over time, since the noncuring vinyl ester resin system was used. In other words, the ionic mobility remained relatively constant throughout the entire time tested. The initial increase in voltage was caused by the infusion of resin and, as in the resistivity cell, the drifting of Cobalt ions. Once the Cobalt salt reached an equilibrium state, the signal stabilized.

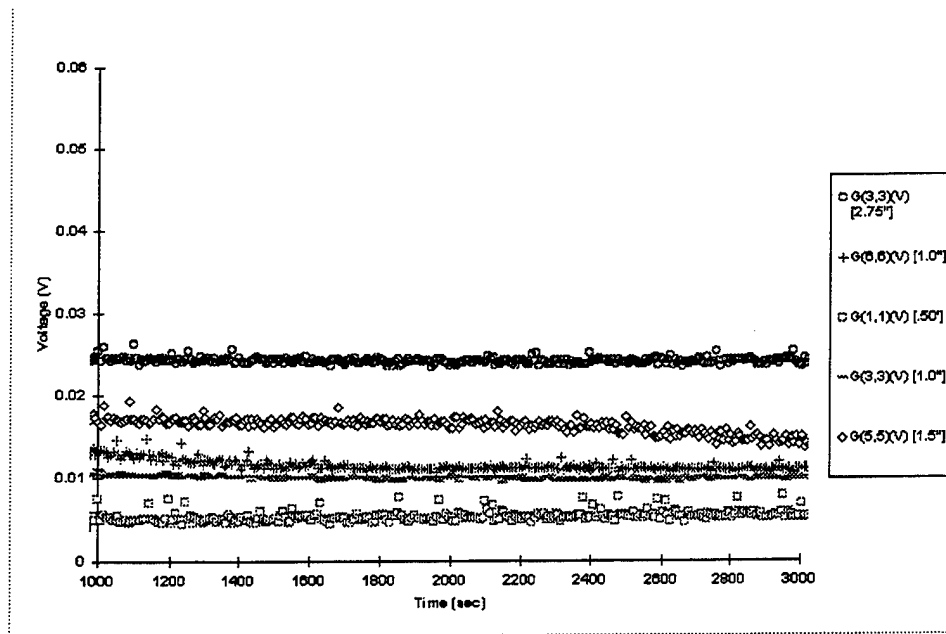


Figure 9. Voltage of SMARTweave Signal for Several Different Hole Diameters.

All four sensor types behaved similarly to the stainless steel mesh; however, there was a significant difference in SMARTweave signals between the four sensor types. Table 3 summarizes the voltage variances. For all hole diameters tested, the stainless steel mesh had the greatest voltage signal. The carbon tow was between 18–20% below that of the mesh. The Cu wire’s voltage signal was consistently 60% below that of the stainless steel mesh. Finally, the stainless steel wire’s voltage remained ~70% below that of the mesh of the same material. The voltage trend seemed to increase with the sensor surface area. However, the exposed surface area alone was not the only explanation for the increased voltage, since the stainless steel wire with a smaller voltage signal had a larger diameter of 0.02 in compared to the diameter of the 28G Cu wire at 0.125 in. The conductivity of Cu is greater than that of stainless steel at $6.0 \times 10^7 (\Omega\text{m})^{-1}$ vs. $1.4 \times 10^6 (\Omega\text{m})^{-1}$, respectively. In this case, the conductivity of the two materials influenced the voltage signal.

4.3.2 Hole Diameter vs. Resistance. The resistance decreased as the hole diameter increased. As shown in Figure 10, the resistance decayed in the uncured resin with the 28G Cu wires as sensors. By extrapolating the curve to a flat region, the minimum horizontal separation distance between sensors may be found. Dependent upon the individual sensor type, each sensor material

Table 3. Comparison of the SMARTweave Signal at Varying Hole Diameters for the Different Sensor Materials

Diameter (in)	Stainless Steel Mesh (mV)	Carbon Tow (mV)	Cu Wire (mV)	Stainless Steel Wire (mV)
0.5	15	12	6	5
1.0	38	21	14	10
1.5	51	40	21	17
3.0	—	—	25	21

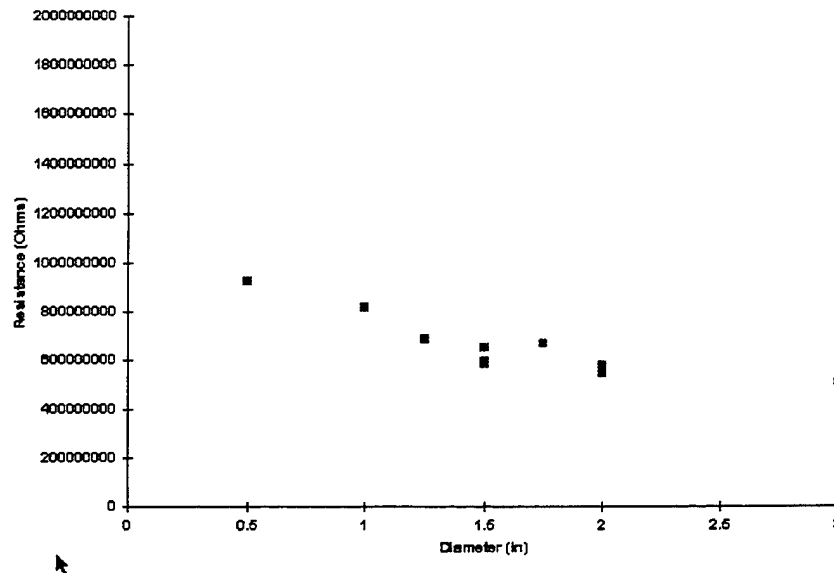


Figure 10. Resistance as Measured by the Cu Sensors in the Varying Hole Diameters.

levels out at different hole diameters. Between 1.0–1.5 in, the Cu wire's resistance decreased by 39%. After this point, a sharp leveling of the curve occurred, and the difference in resistance between 1.5 and 2.0 in was only 2%. For the stainless steel wire, the flattening, or 2% difference in resistances did not occur until the hole diameter reached between 2.0–2.75 in. The resistance continued to decrease for all the hole diameters tested for both the stainless steel mesh and carbon tows.

4.3.3 Effective Area Comparison. Upon further examination, the actual effective area of the node may be determined using equation [1]. As the sensor's exposed surface area increased, so did its effective area. As seen above, the data falls into two main clusters. In the initial slope, or in the region where the hole diameter is less than 1.5 in, the stainless steel mesh and carbon tow have twice the slope than that of the wire combination. Since the stainless steel mesh and carbon tow effective area rose at a much greater rate than that of the two wire sensors, it would be a greater advantage to horizontally separate the first pair by more than 1.5 in. If the upward trend continued past 1.5 in, the greater the horizontal separation, the greater the SMARTweave signal. At this point, it is significant to note (Table 3) that the largest stainless steel wire signal was approximately equal to the smallest stainless steel mesh signal. Also, the Cu wire signal at 1.5 in was almost half that of the carbon tow at the same hole diameter. Therefore, the magnitude of the desired voltage signal would need to be weighed against the grid density for the stainless steel mesh and carbon tows for horizontal separation distances greater than 1.5 in.

In summary, the 0.25-in-wide stainless steel mesh had the highest voltage signal per hole diameter, which indicated the effect of the sensor area. The stainless steel mesh and carbon tow appeared to follow approximately twice the slope of the Cu and stainless steel wire in the effective area-vs.-hole diameter comparison. The Cu wire should be separated by at least 1.5 in to achieve the greatest signal, while the stainless steel wires should be at least 2.0 in to avoid reduced sensor area. It is noted that if increased sensor density is desired, one can place them closer with the understanding that the signal will be decreased.

5. Sensor Area

The sensors individual area was isolated next. To keep vertical and horizontal separation distances constant, carbon tows were used to test the effects of increasing sensor area on the SMARTweave voltage signal.

5.1 Experimental Methods. Three separate 13- × 13-in flat panels were fabricated using six plies of 7781 E-glass. Once again, the tightly woven fabric was used to ensure even separation distances. The sensors were separated by two plies to achieve the greatest voltage signal. Sensors were fabricated using the 4k tows, ranging from 4 to 16k. The increased area sensors were achieved by adhering the individual tows together with uncured Derakane 411-C50. The vinyl ester was first applied to the carbon tows, which were then twisted to ensure a better electrical contact between the individual tows. Next, they were uniformly flattened and placed within the part so that each had a regular thickness along the length/width of the flat plate. Duplicate sensors were placed every 1.5 in ranging from 4 to 16k starting at 1.5 in from all edges. As shown in Figure 11, the nodal area increased along the diagonal from the resin's inlet to the vacuum outlet. Silver conductive paint was used to adhere the tows together over the last 2.5 in on the outside of the vacuum bagging. The part was double vacuum-bagged to insulate it from the metal tool and any electrical noise of the room.

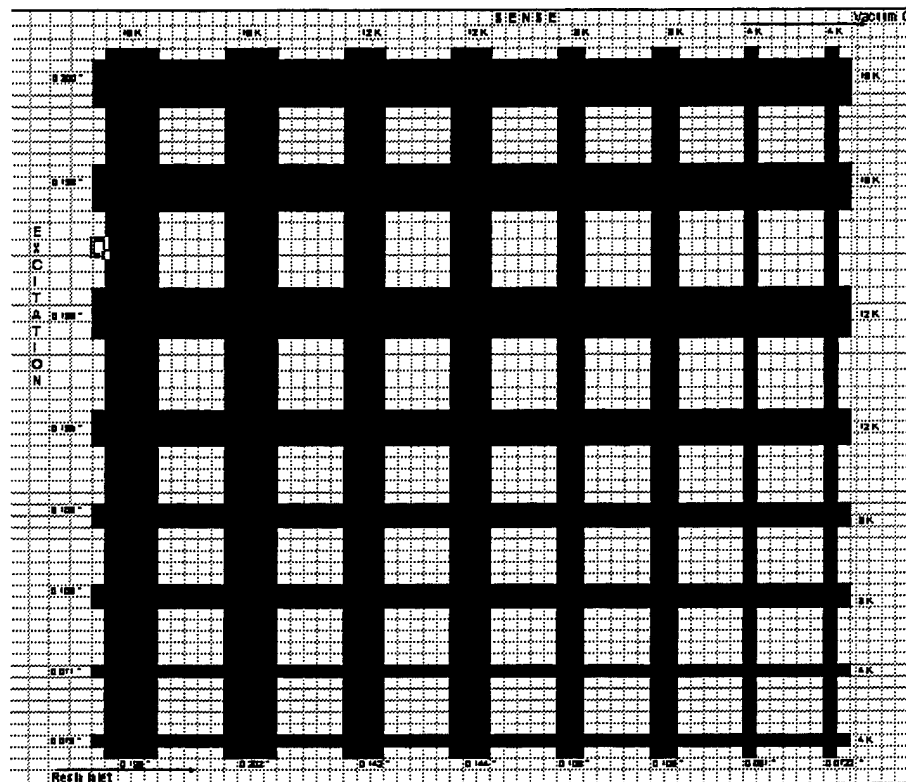


Figure 11. A Schematic of an Experiment to Determine the Effect of Differing Cross-Sectional Areas.

5.2 Results and Discussion. Figure 12 depicts an expanded view of SMARTweave's voltage vs. time along the diagonal of the carbon tow grid. The signal increased with the increasing nodal area. In fact, there is a direct proportionality between the nodal area and SMARTweave signal at the point of infusion, where diffusion limitations from crosslinking are minimal. This area of the curve correlated most directly to the uncured 411-C50/0.2 weight-percent CoNAP resin system. At the largest node (7,7), the initial SMARTweave signal equals 35 mV, while the smallest node (0,0) had a signal 7 times less of 5 mV. Significantly, the total nodal surface area also varied by 7 times. For carbon tows, there appeared to be a direct relationship between the SMARTweave signal and area during the initial stages after infusion.

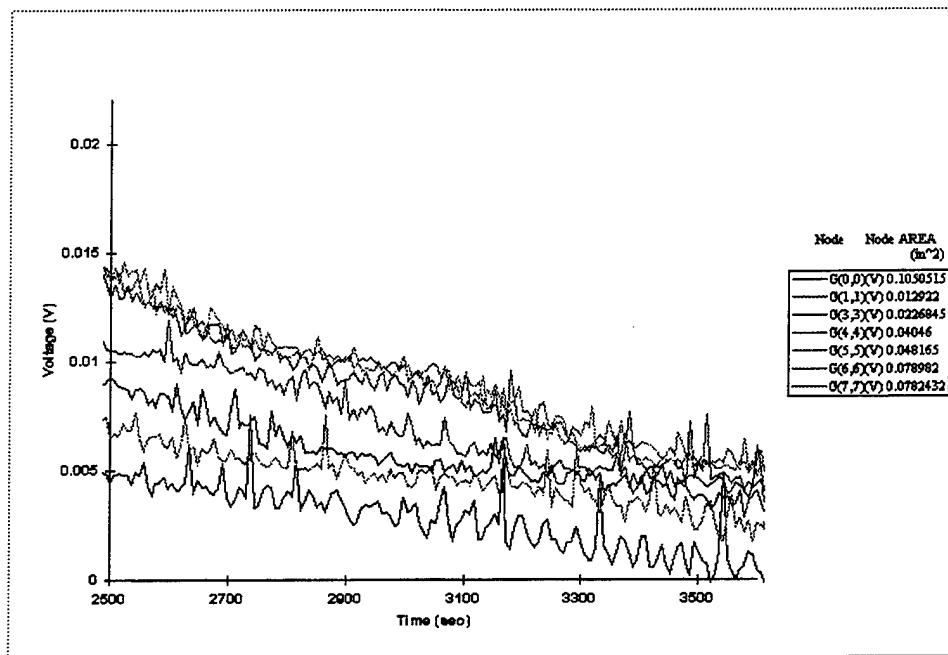


Figure 12. Degradation of Signal as the Area of Conduction Is Reduced.

5.3 Vertical Separation Distance. The effects of vertical separation were investigated in an in-process environment.

5.3.1 Experimental Methods. A 27- × 14-in flat panel was fabricated using 18 total plies of 7781 E-glass. The finely woven 7781 was chosen so that a consistent separation distance could be

achieved. Twenty-two 4k carbon tows with Silver conductive paint on the last 2.5 in were used as the sensor material because of ease of lay-up and lack of coiling properties. Sensors were spaced 1.5 in apart, starting 2 in from all edges. Six excitation sensors were placed on the third ply from the top (all on the same horizontal plane). Sensors 0–7 were separated at increasing increments of two plies ranging from 2–16-ply separation distances. Senses 8–15 had the same setup as 0–7, thereby serving as repeated trials. Each ply of fabric represented 0.011 in. The part was double vacuum-bagged to insulate from the metal tool. The resin system consisted of 1,640-g 411-C50, 34.036-g Trigonox 239A, and 3.444-g CoNAP.

5.3.2 Results and Discussion. In comparing voltage vs. time along an excitation line, no significant difference can be seen in the SMARTweave signal. Repeated trials showed that vertical separation distance does not play a major role in the strength of the SMARTweave signal.

6. Conclusions

The conclusions drawn based on the results will be presented in logical order. To complete the investigation, the criteria defined will be acknowledged.

First, with respect to the horizontal separation distance, it was shown that each sensor material had a range in which the signal increased as the horizontal area increased. Then, at a point, the voltage stops increasing with an increase in area; this area should be used as a minimum spacing to ensure maximum SMARTweave signal. However, if better grid definition is required, it can be accomplished with the understanding that the signal will not be at its maximum potential.

Second, the area of conduction of the sensor type has a direct correlation on the SMARTweave signal. If the cross-sectional area of conduction is increased, by going from a 4k carbon tow to an 8k carbon tow, the signal can be increased.

Third, the vertical separation has been shown to have negligible effects on the SMARTweave signal.

Finally, coupling the seven criteria used to determine the optimal sensor material, carbon tows for glass composite parts appear to be the most effective sensor. Not only is it easy to lay up, but it also produces a strong signal, may easily be woven into the fabric, and can have varied areas. Although the stainless steel wire mesh produces a strong consistent signal, the sharp edges produced a problem in the laying up of the part as well as its cost. Both these issues need to be solved before it is implemented into the SMARTweave package.

7. Future Work

The advancement of the technology associated with the SMARTweave system needs to continue. Work can be done in several areas. First, there are some interesting effects that are a function of the data acquisition system and they need to be understood. Second, further research needs to be put into more and different sensor materials. Finally, a novel idea came out of this research—the ability to use the in-situ sensor grid as a damage detection system.

NO. OF
COPIES ORGANIZATION

2 DEFENSE TECHNICAL
INFORMATION CENTER
DTIC DDA
8725 JOHN J KINGMAN RD
STE 0944
FT BELVOIR VA 22060-6218

1 HQDA
DAMO FDQ
DENNIS SCHMIDT
400 ARMY PENTAGON
WASHINGTON DC 20310-0460

1 DPTY ASSIST SCY FOR R&T
SARD TT F MILTON
RM 3EA79 THE PENTAGON
WASHINGTON DC 20310-0103

1 OSD
OUSD(A&T)/ODDDR&E(R)
J LUPO
THE PENTAGON
WASHINGTON DC 20301-7100

1 CECOM
SP & TRRSTR L COMMCTN DIV
AMSEL RD ST MC M
H SOICHER
FT MONMOUTH NJ 07703-5203

1 PRIN DPTY FOR TCHNLGY HQ
US ARMY MATCOM
AMCDCG T
M FISETTE
5001 EISENHOWER AVE
ALEXANDRIA VA 22333-0001

1 DPTY CG FOR RDE HQ
US ARMY MATCOM
AMCRD
BG BEAUCHAMP
5001 EISENHOWER AVE
ALEXANDRIA VA 22333-0001

1 INST FOR ADVNCD TCHNLGY
THE UNIV OF TEXAS AT AUSTIN
PO BOX 202797
AUSTIN TX 78720-2797

NO. OF
COPIES ORGANIZATION

1 GPS JOINT PROG OFC DIR
COL J CLAY
2435 VELA WAY STE 1613
LOS ANGELES AFB CA 90245-5500

1 ELECTRONIC SYS DIV DIR
CECOM RDEC
J NIEMELA
FT MONMOUTH NJ 07703

3 DARPA
L STOTTS
J PENNELLA
B KASPAR
3701 N FAIRFAX DR
ARLINGTON VA 22203-1714

1 US MILITARY ACADEMY
MATH SCI CTR OF EXCELLENCE
DEPT OF MATHEMATICAL SCI
MDN A MAJ DON ENGEN
THAYER HALL
WEST POINT NY 10996-1786

1 DIRECTOR
US ARMY RESEARCH LAB
AMSRL CS AL TP
2800 POWDER MILL RD
ADELPHI MD 20783-1145

1 DIRECTOR
US ARMY RESEARCH LAB
AMSRL CS AL TA
2800 POWDER MILL RD
ADELPHI MD 20783-1145

3 DIRECTOR
US ARMY RESEARCH LAB
AMSRL CI LL
2800 POWDER MILL RD
ADELPHI MD 20783-1145

ABERDEEN PROVING GROUND

4 DIR USARL
AMSRL CI LP (305)

NO. OF
COPIES ORGANIZATION

1 DIRECTOR
USARL
AMSRL CP CA D SNIDER
2800 POWDER MILL RD
ADELPHI MD 20783

1 COMMANDER
US ARMY ARDEC
AMSTA AR FSE T GORA
PICATINNY ARSENAL NJ
07806-5000

3 COMMANDER
US ARMY ARDEC
AMSTA AR TD
R PRICE
V LINDNER
C SPINELLI
PICATINNY ARSENAL NJ
07806-5000

5 US ARMY TACOM
AMSTA JSK
S GOODMAN
J FLORENCE
AMSTA TR D
B RAJU
L HINOJOSA
D OSTBERG
WARREN MI 48397-5000

5 PM SADARM
SFAE GCSS SD
COL B ELLIS
M DEVINE
W DEMASSI
J PRITCHARD
S HROWNAK
PICATINNY ARSENAL NJ
07806-5000

1 COMMANDER
US ARMY ARDEC
F MCLAUGHLIN
PICATINNY ARSENAL NJ
07806-5000

NO. OF
COPIES ORGANIZATION

5 COMMANDER
US ARMY ARDEC
AMSTA AR CCH
S MUSALLI
P CHRISTIAN
R CARR
M LUCIANO
T LOUCEIRO
PICATINNY ARSENAL NJ
07806-5000

1 COMMANDER
US ARMY ARDEC
AMSTA AR E FENNELL
PICATINNY ARSENAL NJ
07805-5000

1 COMMANDER
US ARMY ARDEC
AMSTA AR CCH
PICATINNY ARSENAL NJ
07806-5000

2 COMMANDER
US ARMY ARDEC
AMSTA AR
PICATINNY ARSENAL NJ
07806-5000

1 COMMANDER
US ARMY ARDEC
AMSTA AR CCH P
J LUTZ
PICATINNY ARSENAL NJ
07806-5000

1 COMMANDER
US ARMY ARDEC
AMSTA AR FSF T
C LIVECCHIA
PICATINNY ARSENAL NJ
07806-5000

1 COMMANDER
US ARMY ARDEC
AMSTA AR QAC T/C
C PATEL
PICATINNY ARSENAL NJ
07806-5000

NO. OF
COPIES ORGANIZATION

2 COMMANDER
US ARMY ARDEC
AMSTA AR M
D DEMELLA
F DIORIO
PICATINNY ARSENAL NJ
07806-5000

3 COMMANDER
US ARMY ARDEC
AMSTA AR FSA
A WARNASH
B MACHAK
C CHIEFA
PICATINNY ARSENAL NJ
07806-5000

8 DIRECTOR
BENET LABORATORIES
AMSTA AR CCB
J KEANE
J BATTAGLIA
J VASILAKIS
G FFIAR
V MONTVORI
J WRZUCHALSKI
R HASENBEIN
AMSTA AR CCB R S SOPOK
WATERVLIET NJ 12189

1 COMMANDER
SMCWV QAE Q B VANINA
BLDG 44 WATERVLIET ARSENAL
WATERVLIET NY 12189-4050

1 COMMANDER
SMCWV SPM T MCCLOSKEY
BLDG 253 WATERVLIET ARSENAL
WATERVLIET NY 12189-4050

1 COMMANDER
SMCWV QA QS K INSCO
WATERVLIET ARSENAL
WATERVLIET NY 12189-4050

1 COMMANDER
US ARMY ARDEC
AMSMC PBM K
PICATINNY ARSENAL NJ
07806-5000

NO. OF
COPIES ORGANIZATION

1 COMMANDER
US ARMY BELVOIR RD&E CTR
STRBE JBC
FORT BELVOIR VA 22060-5606

2 COMMANDER
US ARMY ARDEC
AMSTA AR FSP G
M SCHIKSNIS
D CARLUCCI
PICATINNY ARSENAL NJ
07806-5000

1 US ARMY COLD REGIONS RSRCH
& ENGRNG LAB
P DUTTA
72 LYME RD
HANOVER NH 03755

1 DIRECTOR
USARL
AMSRL WT L D WOODBURY
2800 POWDER MILL RD
ADELPHI MD 20783-1145

3 COMMANDER
US ARMY MISSILE CMD
AMSMI RD W MCCORKLE
AMSMI RD ST P DOYLE
AMSMI RD ST CN T VANDIVER
REDSTONE ARSENAL AL
35898-5247

2 US ARMY RSRCH OFC
A CROWSON
J CHANDRA
PO BOX 12211
RESEARCH TRIANGLE PARK NC
27709-2211

5 PROJECT MANAGER
TMAS
SFAE GSSC TMA
COL PAWLICKI
K KIMKER
E KOPACZ
R ROESER
B DORCY
PICATINNY ARSENAL NJ
07806-5000

NO. OF
COPIES ORGANIZATION

1 PROJECT MANAGER
TMAS
SFAE GSSC TMA SMD
R KOWALSKI
PICATINNY ARSENAL NJ
07806-5000

2 PEO FIELD ARTILLERY SYS
SFAE FAS PM
H GOLDMAN
T MCWILLIAMS
PICATINNY ARSENAL NJ
07806-5000

2 PROJECT MGR CRUSADER
G DELCOCO
J SHIELDS
PICATINNY ARSENAL NJ
07806-5000

2 NASA LANGLEY RSRCH CTR
MS 266
AMSRL VS
W ELBER
F BARTLETT JR
HAMPTON VA 23681-0001

2 COMMANDER
DARPA
J KELLY
B WILCOX
3701 N FAIRFAX DR
ARLINGTON VA 22203-1714

6 COMMANDER
WRIGHT PATTERSON AIR FORCE BASE
WL FIV A MAYER
WL MLBM S DONALDSON
T BENSON TOLLE
C BROWNING
J MCCOY
F ABRAHAMS
2941 P ST STE 1
DAYTON OH 45433

1 NSW CTR
DAHLGREN DIV
CODE G06
DAHLGREN VA 22448

NO. OF
COPIES ORGANIZATION

1 NAVAL RSRCH LAB
CODE 6383
I WOLOCK
WASHINGTON DC 20375-5000

1 OFC OF NAVAL RSRCH
MECH DIV CODE 1132SM
YAPA RAJAPAKSE
ARLINGTON VA 22217

1 NSW CTR
CRANE DIV
M JOHNSON
CODE 20H4
LOUISVILLE KY 40214-5245

1 DAVID TAYLOR RSRCH CTR
SHIP STRUCTURES &
PROTECTION DEPT
J CORRADO CODE 1702
BETHESDA MD 20084

2 DAVID TAYLOR RSRCH CTR
R ROCKWELL
W PHYLLAIER
BETHESDA MD 20054-5000

1 DEFENSE NUCLEAR AGENCY
INNOVATIVE CONCEPTS DIV
DR R ROHR
6801 TELEGRAPH RD
ALEXANDRIA VA 22310-3398

1 DR FRANK SHOUP
EXPEDITIONARY WARFARE DIV N85
2000 NAVY PENTAGON
WASHINGTON DC 20350-2000

1 OFC OF NAVAL RSRCH
D SIEGEL 351
800 N QUINCY ST
ARLINGTON VA 22217-5660

1 JOSEPH H FRANCIS
NSW CTR
CODE G30
DAHLGREN VA 2248

NO. OF COPIES	ORGANIZATION
2	NSW CTR CODE G32 DON WILSON CODE G32 R D COOPER DAHLGREN VA 22448
4	NSW CTR CODE G33 JOHN FRAYSSE ELDRIDGE ROWE TOM DURAN LAURA DE SIMONE DAHLGREN VA 22448
1	COMMANDER NAVAL SEA SYS CMD D LIESE 2531 JEFFERSON DAVIS HWY ARLINGTON VA 22242-5160
1	NSW MARY E LACY CODE B02 17320 DAHLGREN RD DAHLGREN VA 22448
1	NSW TECH LIB CODE 323 17320 DAHLGREN RD DAHLGREN VA 22448
4	DIRECTOR LAWRENCE LIVERMORE NATL LAB R CHRISTENSEN S DETERESA F MAGNESS M FINGER PO BOX 808 LIVERMORE CA 94550
1	LOS ALAMOS NATL LAB F ADDESSIO MS B216 PO BOX 1633 LOS ALAMOS NM 87545
1	LOS ALAMOS NATL LAB R M DAVIS PO BOX 2008 OAK RIDGE TN 27831-6195

NO. OF COPIES	ORGANIZATION
1	PENN STATE UNIV C BAKIS 227 N HAMMOND UNIVERSITY PARK PA 16802
3	UDLP 4800 EAST RIVER RD P JANKE MS170 T GIOVANETTI MS236 B VAN WYK MS389 MINNEAPOLIS MN 55421-1498
4	DIRECTOR SANDIA NATL LAB APPLIED MECHANICS DEPT DIV 8241 W KAWAHARA K PERANO D DAWSON P NIELAN PO BOX 969 LIVERMORE CA 94550-0096
1	BATTELLE C R HARGREAVES 505 KING AVE COLUMBUS OH 43201-2681
1	PACIFIC NORTHWEST LAB M SMITH PO BOX 999 RICHLAND WA 99352
1	LAWRENCE LIVERMORE NATL LAB M MURPHY PO BOX 808 L282 LIVERMORE CA 94550
1	DREXEL UNIV ALBERT S D WANG 32ND & CHESTNUT ST PHILADELPHIA PA 19104
1	NC STATE UNIV CIVIL ENGRNG DEPT W RASDORF PO BOX 7908 RALEIGH NC 27696-7908

NO. OF COPIES	ORGANIZATION
1	PENN STATE UNIV RICHARD MCNITT 227 HAMMOND BLDG UNIVERSITY PARK PA 16802
1	PENN STATE UNIV RENATA ENGEL 245 HAMMOND BLDG UNIVERSITY PARK PA 16801
1	PURDUE UNIV SCHOOL OF AERO & ASTRO CT SUN W LAFAYETTE IN 47907-1282
1	STANFORD UNIV DEPT OF AERONAUTICS & AEROBALLISTICS DURANT BLDG S TSAI STANFORD CA 94305
1	UCLA MANE DEPT ENGR IV H THOMAS HAHN LOS ANGELES CA 90024-1597
2	UNIV OF DAYTON RSRCH INST RAN Y KIM AJIT K ROY 300 COLLEGE PARK AVE DAYTON OH 45469-0168
1	UNIVERSITY OF DAYTON JAMES M WHITNEY COLLEGE PARK AVE DAYTON OH 45469-0240
2	UNIV OF DE CTR FOR COMPOSITE MATERIALS J GILLESPIE M SANTARE 201 SPENCER LAB NEWARK DE 18716

NO. OF COPIES	ORGANIZATION
1	UNIV OF IL AT URBANA CHAMPAIGN NATL CTR FOR COMPOSITE MATERIALS RSRCH 216 TALBOT LAB J ECONOMY 104 S WRIGHT ST URBANA IL 61801
1	UNIV OF KY LYNN PENN 763 ANDERSON HALL LEXINGTON KY 40506-0046
1	UNIV OF UT DEPT OF MECH & INDUSTRIAL ENGR S SWANSON SALT LAKE CITY UT 84112
3	THE UNIV OF TX AT AUSTIN CTR FOR ELECTROMECHANICS J PRICE A WALLS J KITZMILLER 10100 BURNET RD AUSTIN TX 78758-4497
3	VPI AND STATE UNIV DEPT OF ESM M W HYER K REIFSNIDER R JONES BLACKSBURG VA 24061-0219
1	UNIV OF MD DR ANTHONY J VIZZINI DEPT OF AEROSPACE ENGRNG COLLEGE PARK MD 20742
1	AAI CORP DR T G STASTNY PO BOX 126 HUNT VALLEY MD 21030-0126
1	JOHN HEBERT PO BOX 1072 HUNT VALLEY MD 21030-0126

NO. OF
COPIES ORGANIZATION

1 ARMTEC DEFENSE PRODUCTS
STEVE DYER
85 901 AVE 53
PO BOX 848
COACHELLA CA 92236

2 ADVANCED COMP MATERIALS CORP
P HOOD
J RHODES
1525 S BUNCOMBE RD
GREER SC 29651-9208

1 SAIC
DAN DAKIN
2200 POWELL ST STE 1090
EMERYVILLE CA 94608

1 SAIC
MILES PALMER
2109 AIR PARK RD S E
ALBUQUERQUE NM 87106

1 SAIC
ROBERT ACEBAL
1225 JOHNSON FERRY RD STE 100
MARIETTA GA 30068

1 SAIC
DR GEORGE CHRYSSOMALLIS
3800 W 80TH STREET
STE 1090
BLOOMINGTON MN 55431

4 ALLIANT TECHSYSTEMS INC
C CANDLAND
R BECKER
L LEE
R LONG
D KAMDAR
G KASSUELKE
600 2ND ST NE
HOPKINS MN 55343-8367

1 AMOCO PERFORMANCE PRODUCTS INC
M MICHNO JR
4500 MCGINNIS FERRY RD
ALPHARETTA GA 30202-3944

NO. OF
COPIES ORGANIZATION

1 APPLIED COMPOSITES
W GRISCH
333 NORTH SIXTH ST
ST CHARLES IL 60174

1 BRUNSWICK DEFENSE
T HARRIS
STE 410
1745 JEFFERSON DAVIS HWY
ARLINGTON VA 22202

1 PROJECTILE TECHNOLOGY INC
515 GILES ST
HAVRE DE GRACE MD 21078

1 CUSTOM ANALYTICAL ENGR SYS INC
A ALEXANDER
13000 TENSOR LANE NE
FLINTSTONE MD 21530

1 NOESIS INC
ALLEN BOUTZ
1110 N GLEBE RD STE 250
ARLINGTON VA 22201-4795

1 ARROW TECH ASSO
1233 SHELBURNE RD STE D 8
SOUTH BURLINGTON VT 05403-7700

1 NSWC
R HUBBARD G33 C
DAHLGREN DIV
DAHLGREN VA 22448-5000

5 GEN CORP AEROJET
D PILLASCH
T COULTER
C FLYNN
D RUBAREZUL
M GREINER
1100 WEST HOLLYVALE ST
AZUSA CA 91702-0296

<u>NO. OF</u> <u>COPIES</u>	<u>ORGANIZATION</u>
7	CIVIL ENGR RSRCH FOUNDATION H BERNSTEIN PRESIDENT C MAGNELL K ALMOND R BELLE M WILLETT E DELO B MATTES 1015 15TH ST NW STE 600 WASHINGTON DC 20005
1	NIST STRCTRE & MCHNCS GROUP POLYMER DIV POLYMERS RM A209 GREGORY MCKENNA GAITHERSBURG MD 20899
1	DUPONT COMPANY COMPOSITES ARAMID FIBERS S BORLESKE DVLPMNT MGR CHESNUT RUN PLAZA PO BOX 80702 WILMINGTON DE 19880-0702
1	GENERAL DYNAMICS LAND SYSTEMS DIVISION D BARTLE PO BOX 1901 WARREN MI 48090
3	HERCULES INC R BOE F POLICELLI J POESCH PO BOX 98 MAGNA UT 84044
3	HERCULES INC G KUEBELER J VERMEYCHUK B MANDERVILLE JR HERCULES PLZ WILMINGTON DE 19894
1	HEXCEL M SHELENDICH 11555 DUBLIN BLVD PO BOX 2312 DUBLIN CA 94568-0705

<u>NO. OF</u> <u>COPIES</u>	<u>ORGANIZATION</u>
1	IAP RESEARCH INC A CHALLITA 2763 CULVER AVE DAYTON OH 45429
5	INSTITUTE FOR ADVANCED TECH T KIEHNE H FAIR P SULLIVAN W REINECKE I MCNAB 4030 2 W BRAKER LN AUSTIN TX 78759
1	INTEGRATED COMPOSITE TECH H PERKINSON JR PO BOX 397 YORK NEW SALEM PA 17371-0397
1	INTERFEROMETRICS INC R LARRIVA VICE PRESIDENT 8150 LEESBURG PIKE VIENNA VA 22100
1	AEROSPACE RES & DEV (ASRDD) CORP D ELDER PO BOX 49472 COLORADO SPRINGS CO 80949-9472
1	PM ADVANCED CONCEPTS LORAL VOUGHT SYSTEMS J TAYLOR PO BOX 650003 MS WT 21 DALLAS TX 76265-0003
2	LORAL VOUGHT SYSTEMS G JACKSON K COOK 1701 W MARSHALL DR GRAND PRAIRIE TX 75051
1	BRIGS CO JOE BACKOFEN 2668 PETERBOROUGH ST HERDON VA 22071-2443

NO. OF
COPIES ORGANIZATION

1 SOUTHWEST RSRCH INSTITUTE
JACK RIEGEL
ENGRG & MTRL SCIENCES DIV
6220 CULEBRA RD
PO DRAWER 28510
SAN ANTONIO TX 78228-0510

1 ZERNOW TECHNICAL SERVICES
LOUIS ZERNOW
425 W BONITA AVE SUITE 208
SAN DIMAS CA 91773

1 ROBERT EICHELBERGER
CONSULTANT
409 W CATHERINE ST
BEL AIR MD 21014-3613

1 DYNA EAST CORPORATION
PEI CHI CHOU
3201 ARCH ST
PHILADELPHIA PA 19104-2711

2 MARTIN MARIETTA CORP
P DEWAR
L SPONAR
230 EAST GODDARD BLVD
KING OF PRUSSIA PA 19406

2 OLIN CORPORATION
FLINCHBAUGH DIV
E STEINER
B STEWART
PO BOX 127
RED LION PA 17356

1 OLIN CORPORATION
L WHITMORE
10101 9TH ST NORTH
ST PETERBURG FL 33702

1 RENNSAELER PLYTCHNC INST
R B PIPES
PRESIDENT OFC
PITTSBURGH BLDG
TROY NY 12180-3590

1 SPARTA INC
J GLATZ
9455 TOWNE CTR DRIVE
SAN DIEGO CA 92121-1964

NO. OF
COPIES ORGANIZATION

2 UNITED DEFENSE LP
P PARA
G THOMAS
1107 COLEMAN AVE BOX 367
SAN JOSE CA 95103

1 MARINE CORPS SYSTEMS CMD
PROGRAM MGR GROUND WPNS
COL RICK OWEN
2083 BARNETT AVE SUITE 315
QUANTICO VA 22134-5000

1 OFFICE OF NAVAL RES
J KELLY
800 NORTH QUINCEY ST
ARLINGTON VA 22217-5000

2 NSWC
CARDEROCK DIV
R CRANE CODE 2802
C WILLIAMS CODE 6553
3A LEGGETT CIR
ANNAPOLIS MD 21402

5 SIKORSKY
H BUTTS
T CARSTENSAN
B KAY
S GARBO
J ADELMANN
6900 MAIN ST
PO BOX 9729
STRATFORD CT 06601-1381

1 D ADAMS
U WYOMING
PO BOX 3295
LARAMIE WY 82071

1 MICHIGAN ST UNIVERSITY
R AVERILL
3515 EB MSM DEPT
EAST LANSING MI 48824-1226

1 AMOCO POLYMERS
J BANISAUKAS
4500 MCGINNIS FERRY RD
ALPHARETTA GA 30005

NO. OF COPIES	ORGANIZATION
1	HEXCEL T BITZER 11711 DUBLIN BLVD DUBLIN CA 94568
1	BOEING R BOHLMANN PO BOX 516 MC 5021322 ST LOUIS MO 63166-0516
1	NAVSEA OJRI G CAMPONESCHI 2351 JEFFERSON DAVIS HWY ARLINGTON VA 22242-5160
1	LOCKHEED MARTIN R FIELDS 1195 IRWIN CT WINTER SPRINGS FL 32708
1	USAF WL/MLS OL A HAKIM 5225 BAILEY LOOP 243E MCCLELLAN AFB CA 55552
1	PRATT & WHITNEY D HAMBRICK 400 MAIN ST MS 114 37 EAST HARTFORD CT 06108
1	DOUGLAS PRODUCTS DIV BOEING L J HART-SMITH 3855 LAKEWOOD BLVD D800-0019 LONG BEACH CA 90846-0001
1	MIT P LAGACE 77 MASS AVE CAMBRIDGE MA 01887
1	NASA LANGLEY J MASTERS MS 389 HAMPTON VA 23662-5225

NO. OF COPIES	ORGANIZATION
1	CYTEC M LIN 1440 N KRAEMER BLVD ANAHEIM CA 92806
2	BOEING ROTORCRAFT P MINGURT P HANDEL 800 B PUTNAM BLVD WALLINGFORD PA 19086
2	FAA TECH CENTER D OPLINGER AAR 431 P SHYPRYKEVICH AAR 431 ATLANTIC CITY INTL AIRPORT NJ 08405
1	NASA LANGLEY RC CC POE MS 188E NEWPORT NEWS VA 23608
1	LOCKHEED MARTIN S REEVE 8650 COBB DR D/73-62 MZ 0648 MARIETTA GA 30063-0648
1	WL/MLBC E SHINN 2941 PST STE 1 WRIGHT PATTERSON AFB OH 45433-7750
2	IIT RESEARCH CENTER D ROSE 201 MILL ST ROME NY 13440-6916
1	MATERIALS SCIENCES CORP BW ROSEN 500 OFFICE CENTER DR STE 250 FT WASHINGTON PA 19034
1	DOW UT S TIDRICK 15 STERLING DR WALLINGFORD CT 06492

NO. OF
COPIES ORGANIZATION

3 TUSKEGEE UNIVERSITY
MATERIALS RSRCH LAB
SCHOOL OF ENGR & ARCH
S JEELANI
H MAHFUZ
U VAIDYA
TUSKEGEE AL 36088

4 NIST
R PARNAS
J DUNKERS
M VANLANDINGHAM
D HUNSTON
POLYMERS DIVISION
GAITHERSBURG MD 20899

2 NORTHROP GRUMMAN
ENVIRONMENTAL PROGRAMS
R OSTERMAN
8900 E WASHINGTON BLVD
PICO RIVERA CA 90660

1 OAK RIDGE NATL LAB
A WERESZCZAK
BLDG 4515 MS 6069
PO BOX 2008
OAKRIDGE TN 37831-6064

1 COMMANDER
US ARMY ARDEC
T SACHAR
INDUSTRIAL ECOLOGY CTR
BLDG 172
PICATINNY ARSENAL NJ
07806-5000

1 COMMANDER
USA ATCOM
AVIATION APPLIED TECH DIR
J SCHUCK
FORT EUSTIS VA 23604-1104

1 COMMANDER
US ARMY ARDEC
AMSTA AR SRE D YEE
PICATINNY ARSENAL NJ
07806-5000

NO. OF
COPIES ORGANIZATION

7 COMMANDER
US ARMY ARDEC
AMSTA AR CCH B
B KONRAD
E RIVERA
G EUSTICE
S PATEL
G WAGNECZ
R SAYER
F CHANG
BLDG 65
PICATINNY ARSENAL NJ
07806-5000

1 COMMANDER
US ARMY ARDEC
AMSTA AR QAC T
D RIGOGLIOSO
BLDG 354 M829E3 IPT
PICATINNY ARSENAL NJ
07806-5000

ABERDEEN PROVING GROUND

75 DIR USARL
AMSRL CI C NIETUBICZ 394
AMSRL CI C W STUREK 1121
AMSRL CI CB R KASTE 394
AMSRL CI S A MARK 309
AMSRL SL B
AMSRL SL BA
AMSRL SL BE D BELY 328
AMSRL WM B
A HORST 390A
E SCHMIDT 390A
AMSRL WM BE
G KELLER 390
C LEVERITT 390
D KOOKER 390A
AMSRL WM BC
P PLOSTINS 390
D LYON 390
J NEWILL 390
S WILKERSON 390
AMSRL WM BD
R FIFER 390
B FORCH 390A
R PESCE-RODRIGUEZ 390
B RICE 390A

NO. OF
COPIES ORGANIZATION

AMSRL WM
 D VIECHNICK 4600
 G HAGNAUER 4600
 J MCCAULEY 4600
 AMSRL WM MA
 R SHUFORD 4600
 S MCKNIGHT 4600
 AMSRL WM MB
 B BURNS 4600
 W DRYSDALE 4600
 J BENDER 4600
 T BLANAS 4600
 T BOGETTI 4600
 R BOSSOLI 120
 L BURTON 4600
 J CONNORS 4600
 S CORNELISON 120
 P DEHMER 4600
 R BOOLEY 4600
 B FINK 4600
 G GAZONAS 4600
 S GHIORSE 4600
 D GRANVILLE 4600
 D HOPKINS 4600
 C HOPPEL 4600
 D HENRY 4600
 R KASTE 4600
 R KLINGER 4600
 M LEADORE 4600
 R LIEB 4600
 E RIGAS 4600
 D SPAGNUOLO 4600
 W SPURGEON 4600
 J TZENG 4600
 AMSRL WM MB ALC
 A ABRAHAMIAN
 M BERMAN
 A FRYDMAN
 T LI
 W MCINTOSH
 E SZYMANSKI
 AMSRL WM MC T HYNES 4600
 AMSRL WM MD W ROY 4600
 AMSRL WM ME R ADLER 4600
 AMSRL WM T W MORRISON 309
 AMSRL WM TA
 W GILLICH 393
 W BRUCHEY 393
 T HAVEL 393
 AMSRL WM TC

R COATES 309
 W DE ROSSET 309
 AMSRL WM TD
 T CHOU 4600
 D DIETRICH 309
 A DAS GUPTA 309
 AMSRL WM TE J POWELL 120
 AMSRL WM BA
 F BRANDON 120
 W D AMICO 120
 AMSRL WM BB J BORNSTEIN 120
 AMSRL WM BC A ZIELINSKI 390
 AMSRL WM BF J LACETERA 120

REPORT DOCUMENTATION PAGE			Form Approved OMB No. 0704-0188	
<small>Public reporting burden for this collection of information is estimated to average 1 hour per response, including the time for reviewing instructions, searching existing data sources, gathering and maintaining the data needed, and completing and reviewing the collection of information. Send comments regarding this burden estimate or any other aspect of this collection of information, including suggestions for reducing this burden, to Washington Headquarters Services, Directorate for Information Operations and Reports, 1215 Jefferson Davis Highway, Suite 1204, Arlington, VA 22202-4302, and to the Office of Management and Budget, Paperwork Reduction Project(0704-0188), Washington, DC 20503.</small>				
1. AGENCY USE ONLY (Leave blank)		2. REPORT DATE May 1998	3. REPORT TYPE AND DATES COVERED Final, Dec 95 - Oct 96	
4. TITLE AND SUBTITLE Investigation of Geometric Effects on the SMARTweave Signal			5. FUNDING NUMBERS COMP02	
6. AUTHOR(S) Clarissa J. DuBois, William O. Ballata, and Shawn M. Walsh				
7. PERFORMING ORGANIZATION NAME(S) AND ADDRESS(ES) U.S. Army Research Laboratory ATTN: AMSRL-WM-MD Aberdeen Proving Ground, MD 21005-5069			8. PERFORMING ORGANIZATION REPORT NUMBER ARL-TR-1675	
9. SPONSORING/MONITORING AGENCY NAMES(S) AND ADDRESS(ES)			10. SPONSORING/MONITORING AGENCY REPORT NUMBER	
11. SUPPLEMENTARY NOTES				
12a. DISTRIBUTION/AVAILABILITY STATEMENT Approved for public release; distribution is unlimited.			12b. DISTRIBUTION CODE	
13. ABSTRACT (Maximum 200 words) <p>SMARTweave or Sensors Mounted As Roving Threads is an electrical grid comprised of orthogonal noncontacting conductive filaments used primarily to monitor the resin flow in the manufacturing of liquid-molded composite materials. It works on the principles of the half Wheatstone bridge and ionic mobility. It has been successfully demonstrated as a technology, but now the challenge is to characterize the system and its behaviors. The variables addressed in this report are basically geometric in nature. The following will each be investigated: the sensor materials and their perpendicular area of conduction, the separation from one node to the next in the horizontal plane, and the separation from one lead to the next in the vertical plane. Results are presented regarding the SMARTweave sensor materials and signals. The results on horizontal spacing, the area of conduction, and vertical separation will be presented.</p>				
14. SUBJECT TERMS SMARTweave, process sensor, resin transfer molding			15. NUMBER OF PAGES 25	
			16. PRICE CODE	
17. SECURITY CLASSIFICATION OF REPORT UNCLASSIFIED	18. SECURITY CLASSIFICATION OF THIS PAGE UNCLASSIFIED	19. SECURITY CLASSIFICATION OF ABSTRACT UNCLASSIFIED	20. LIMITATION OF ABSTRACT UL	

INTENTIONALLY LEFT BLANK.

USER EVALUATION SHEET/CHANGE OF ADDRESS

This Laboratory undertakes a continuing effort to improve the quality of the reports it publishes. Your comments/answers to the items/questions below will aid us in our efforts.

1. ARL Report Number/Author ARL-TR-1675 (DuBois) Date of Report May 1998

2. Date Report Received _____

3. Does this report satisfy a need? (Comment on purpose, related project, or other area of interest for which the report will be used.) _____

4. Specifically, how is the report being used? (Information source, design data, procedure, source of ideas, etc.) _____

5. Has the information in this report led to any quantitative savings as far as man-hours or dollars saved, operating costs avoided, or efficiencies achieved, etc? If so, please elaborate. _____

6. General Comments. What do you think should be changed to improve future reports? (Indicate changes to organization, technical content, format, etc.) _____

CURRENT
ADDRESS

Organization

Name

E-mail Name

Street or P.O. Box No.

City, State, Zip Code

7. If indicating a Change of Address or Address Correction, please provide the Current or Correct address above and the Old or Incorrect address below.

OLD
ADDRESS

Organization

Name

Street or P.O. Box No.

City, State, Zip Code

(Remove this sheet, fold as indicated, tape closed, and mail.)
(DO NOT STAPLE)